Geoscience Frontiers xxx (xxxx) xxx

HOSTED BY

ELSEVIER

Contents lists available at ScienceDirect

Geoscience Frontiers

journal homepage: www.elsevier.com/locate/gsf

Research paper

Source identification and global implications of black carbon

Erika P. Blanco-Donado [a,*], Ismael L. Schneider [a], Paulo Artaxo [a,b], Jesus Lozano-Osorio [a], Luana Portz [a], Marcos L.S. Oliveira [a,c]

[a] Department of Civil and Environmental, Universidad de la Costa, CUC, Barranquilla, 080002, Colombia
[b] Department of Applied Physics, Institute of Physics, University of São Paulo, SP 05508-220, Brazil
[c] Universidad de Lima, Avenida Javier Prado Este 4600, Santiago de Surco 1503, Peru

ARTICLE INFO

Article history:
Received 12 October 2020
Received in revised form 5 January 2021
Accepted 13 January 2021
Available online xxxx

Handling Editor: M. Santosh

Keywords:
Air pollution
Black carbon
Spatial distribution
Source apportionment
Absorption Ångström exponent

ABSTRACT

Black carbon (BC) is one of the short-lived air pollutants that contributes significantly to aerosol radiative forcing and global climate change. It is emitted by the incomplete combustion of fossil fuels, biofuels, and biomass. Urban environments are quite complex and thus, the use of mobile jointly with fixed monitoring provides a better understanding of the dynamics of BC distribution in such areas. The present study addresses the measurement of BC concentration using real-time mobile and ambient monitoring in Barranquilla, an industrialized urban area of the Colombian Caribbean. A microaethalometer (MA200) and an aethalometer (AE33) were used for measuring the BC concentration. The absorption Ångström exponent (AAE) values were determined for the study area, for identifying the BC emission sources. The results of the ambient sampling show that vehicle traffic emissions prevail; however, the influence of biomass burning was also observed. The mean ambient BC concentration was found to be 1.04 ± 1.03 μg/m^3 and varied between 0.5 and 4.0 μg/m^3. From the mobile measurements obtained in real traffic conditions on the road, a much higher average value of 16.1 ± 16.5 μg/m^3 was measured. Many parts of the city showed BC concentrations higher than 20 μg/m^3. The spatial distribution of BC concentration shows that vehicle emissions and traffic jams, a consequence of road and transport infrastructure, are the factors that most affect the BC concentration. A comparison of results obtained from two aethalometers indicates that the concentrations measured by MA200 are 9% lower than those measured by AE33. The AAE obtained was found to vary between 1.1 and 1.6, indicating vehicular emissions as the most crucial source. In addition, it was observed that the BC concentration on working days was 2.5 times higher than on the weekends in the case of mobile monitoring and 1.5 times higher in the case of ambient monitoring.

1. Introduction

Human and environmental health is always exposed to atmospheric nanoparticles (NPs) and ultra-fine particles (UFPs) through breathe, ingestion, dermal interaction, and eyes connections (Martinello et al., 2014; Saikia et al., 2014, 2018; Schneider et al., 2016; Duarte et al., 2019; Rojas et al., 2019; Madureira et al., 2020; Silva et al., 2020a, 2020b, 2020c, 2020d). In general black carbon (BC) is an aerosol product of incomplete combustion of fossil fuels, biofuel or biomass, generally originated from anthropogenic activities such as emissions from vehicles, industries, and burning of solid waste, among others (Bond et al., 2013). It is mostly used as an indicator of combustion sources since its physical properties, and airborne concentration varies depending on the type of fuel used, combustion characteristics, and meteorology (Schneider et al., 2015; Agudelo-Castañeda et al., 2016, 2017; Sehn et al., 2016; Evans et al., 2017; Saturno et al., 2018; Ramírez et al., 2019). The study of BC concentration and its control depends on the evidence of the negative impact that BC has on people's health in terms of the alterations it causes in respiratory and cardiovascular functions (de Oliveira Alves et al., 2011; de Oliveira Alves et al., 2015; de Oliveira Alves et al., 2017; Wang et al., 2016; Becerril-Valle et al., 2017). BC aerosol particles are present mostly in the fine mode ($PM_{2.5}$) and can be inhaled and get deposited in the lungs quite efficiently (Gong et al., 2019). BC is considered to be more harmful to people than other particle components such as PM_{10} and $PM_{2.5}$ particulate materials (de Oliveira Alves et al., 2012; Li et al., 2015). BC also has an important impact on the climate as it is responsible for a positive radiative forcing (warming) of 0.6 W/m^2 (Boucher et al., 2013). This value is about one-quarter of the CO_2 radiative forcing, a very significant figure. BC also has an impact on the increase of snow melting when it gets deposited over snow (US EPA, 2012).

In Latin America and the Caribbean, the main sources of BC emission are vehicular traffic in urban areas and biomass burning from deforestation, cooking, and heating (Artaxo et al., 2013; Brito et al., 2013). Therefore, knowledge on BC concentration and its sources is important in

* Corresponding author.
E-mail address: eblanco5@cuc.edu.co (E.P. Blanco-Donado).

https://doi.org/10.1016/j.gsf.2021.101149

order to establish strategies for reducing emissions and their atmospheric concentrations which, in turn, would contribute to the reduction of exposure of people to BC and provide short-term climate benefits (Krecl et al., 2014; Reddington et al., 2015; Scott et al., 2018).

In urban areas, atmospheric BC is usually measured by employing light absorption techniques such as aethalometers (Rizzo et al., 2011; Dumka et al., 2013; Saturno et al., 2017; Mousavi et al., 2019), multi-angle absorption photometry (MAAP) (Petzold et al., 2005; Coen et al., 2010), and remote sensing tools (Zhu et al., 2017). However, BC monitoring in urban areas is challenging due to the large spatial variability of the pollutants which, in turn, is dependent on the variability in traffic density, street topology, and distance to the sources (Van Poppel et al., 2013). The alternative technique of mobile sampling allows the acquisition of data in terms of air quality with a high spatial and temporal resolution in a complex urban environment. It thus provides vital information for assessing the spatial variability of pollutants with a limited number of instruments in a short duration. This method can be used for air quality mapping in an urban neighborhood (Targino et al., 2018), identification of hot spot areas having a high BC concentration (Targino et al., 2016), and also exposure evaluation of cyclists (Franco et al., 2016), pedestrians (Morales Betancourt et al., 2017), and drivers (Liu et al., 2019a; Liu et al., 2019b), in order to obtain information on exposure levels in them (Okokon et al., 2017).

This study aimed to map the geographical distribution of BC in a medium-sized urban area, as well as explore the use of AAE in the identification of BC sources. BC concentration was determined using both ambient real-time monitoring and mobile monitoring in the industrialized city of Barranquilla in the Colombian Caribbean. The chosen mobile monitoring route was characterized by a mixture of residential, industrial, and commercial areas, with different traffic density. In addition to BC concentration mapping, the absorption Ångström exponents (AAEs) (Bergstrom et al., 2002; Bond and Bergstrom, 2006) were determined to provide information on the identification of BC sources. A comparison between the two aethalometers used in this study was also carried out to ensure the quality of the information obtained.

2. Methodology

2.1. Study area

Barranquilla (10°59′16"N, 74°47′20"W) is the capital of the department of Atlántico in Colombia located on the Caribbean coast at an elevation of 18 m above sea level and has a population of approximate 1.2 million inhabitants. It has an area of 154 km^2 and an annual average temperature of 27 °C (between 23 and 31 °C). The average annual precipitation is 767 mm, and the predominant wind direction is north-northeast (NNE). The climate of the city is classified as a dry tropical type and is characterized by a wet period from April to November and a dry period from December to March.

Barranquilla is officially referred to as a special, industrial, and a port district. It is a coastal city consisting of fixed industrial sources, mainly those dedicated to the elaboration of food and drink products, chemical products, substances, and basic metallurgical products manufacturing, on which part of the local economy depends (Table S1, Supplementary Data). This city has a vehicle fleet consisting of private cars (~126,000), followed by motorcycles (~31,000), public cars (~15,000), and buses for public transport (~8000). There is no emission control system for vehicular emissions in Barranquilla (Table S2, Supplementary Data).

For the mobile sampling of BC, a route was selected in order to consider different types of activities along the route (i.e., consisting of commercial, industrial, and residential sectors) as well as diversity in road configuration and vehicle density. The chosen route borders the entire periphery of the city, as can be seen from Fig. 1. Therefore, the BC data collected in this work represents the various environments and influences of different sources in the urban area of Barranquilla.

The location of the fixed site (Fig. 1) used for ambient BC sampling has a contribution from multiple pollutant emission sources. It is located at the top of a 5-floor building of the Universidad de la Costa, in a residential area near busy roads and industrial areas. Due to its geographical location and predominance of the NNE wind direction, the BC found in this area also contains the contribution from biomass burning from the nearby mangrove nature reserve of Isla Salamanca Natural Park, an important area for bird conservation and declared as a biosphere reserve by UNESCO. In this area, frequent biomass burning is observed during March and June.

2.2. Sampling and data processing

A portable micro-aethalometer of model MA200 (AethLabs, San Francisco, USA) was used for carrying out the BC mobile monitoring campaigns. This instrument measures a change in light attenuation in a filter at five wavelengths: 375 nm (ultraviolet), 470 nm (blue), 528 nm (green), 625 nm (red) and 880 nm (infrared), with mass absorption cross-sections (MACs) of 24.069, 19.070, 17.028, 14.091, and 10.120 m^2/g respectively, provided by the manufacturer. In addition, it incorporates the dual-spot method to compensate for the absorption effects of aerosol loading (Boniardi et al., 2019; Madueño et al., 2019; Wang et al., 2020). The portable micro-aethalometer follows the same measurement principle as the AE33 aethalometer, where the aerosol particles are continually sampled on the filter and the optical attenuation is measured with high time resolution. Attenuation is measured on two spots with different sample flows and on the reference spot without the flow. The BC mass concentration is calculated from the change in optical attenuation of the different wavelengths in the selected time interval using the mass absorption cross section (Drinovec et al., 2015). Other authors have addressed the model working principle of the aethalometer in more detail (Dumka et al., 2013; Becerril-Valle et al., 2017; Martinsson et al., 2017; Zotter et al., 2017).

The mobile platform consisted of a car equipped with a global positioning system (GPS) (Garmin model 450) and a portable micro-aethalometer, collecting the information in time intervals of 1 min, with a flow rate of 150 mL/min, and a car speed of approximately 30 km/h. The micro-aethalometer was outside the vehicle, with the $PM_{2.5}$ cyclone attached to support located on the left side window at an approximate height of 2 m above the road surface.

The steps established by Targino et al. (2016) and the manufacturer's suggestions (AethLabs) were followed for preparing the portable micro-aethalometer before each sampling campaign. The data discarded by the GPS was examined for detecting any erroneous geolocations as well as, the speed and distance of each mobile sampling campaign. The design of the sampling route was characterized by different types of activities on the periphery of Barranquilla city (in the commercial, industrial, and residential areas). The samples from a total of 13 complete routes were taken between May to June 2019. Each sampling campaign started at 14:00 and lasted for about 2 h. This schedule was selected by considering a period which the weather conditions remain rather uniform, with low variations in the boundary layer height that would minimize the interference of the meteorological variables. The sampling was performed during days of no precipitation. In order to calculate the AAEs, the BC data obtained with the micro-aethalometer was processed by applying a polynomial regression smoothing method to the measurements at the five wavelengths.

In the ambient BC monitoring campaign at a fixed site at the Universidad de la Costa, an AE33 aethalometer (Magee Scientific Company, Berkley, USA) was used to carry out continuous measurements from May to June 2019. This period corresponds to the dry season. The data was recorded at time intervals of 1 min and a flow rate of 5 L/min. Drinovec et al. (2015) have previously described the characteristics of the instrument. An aerosol dryer was used to make sure that the relative humidity is kept constant at ≤35%.

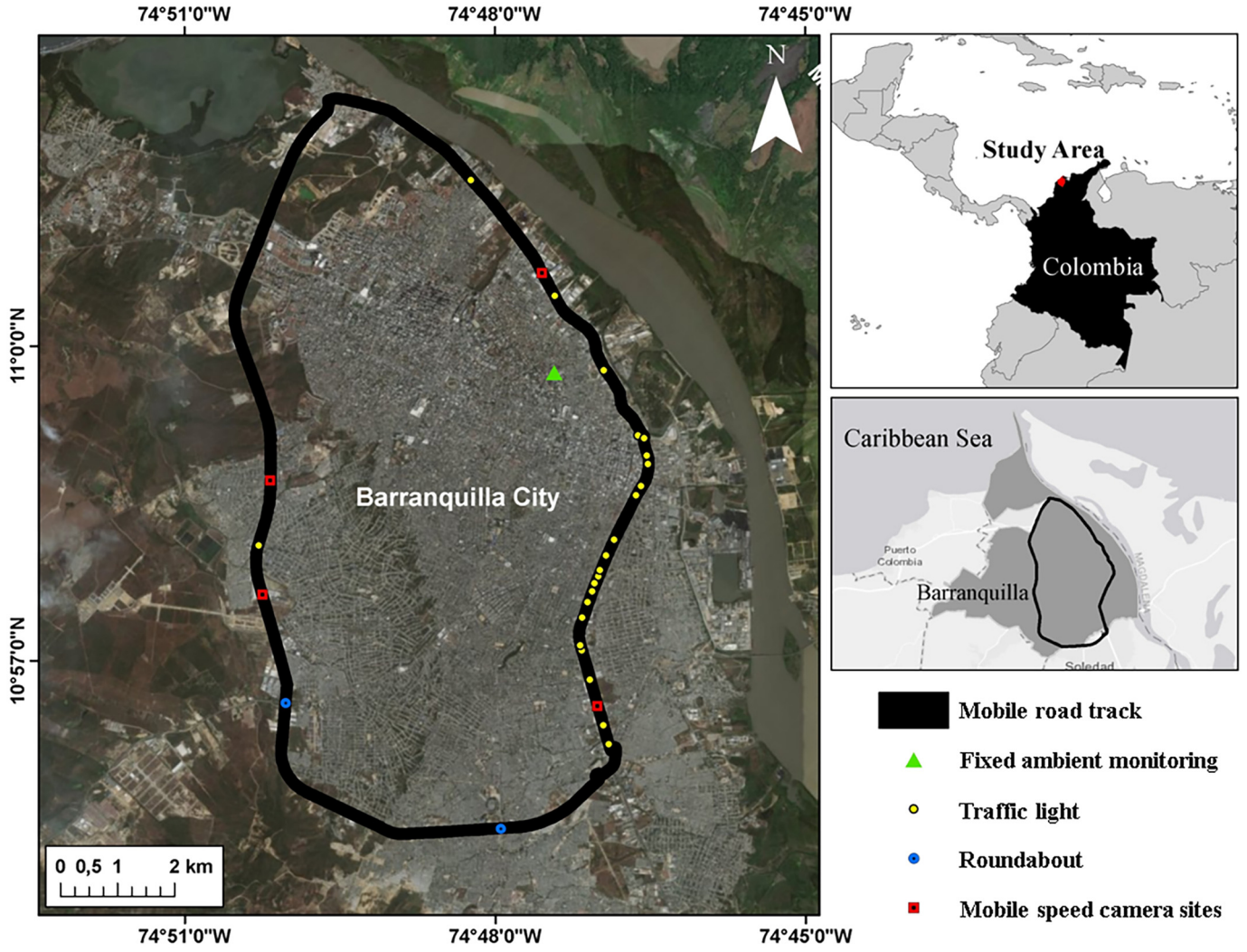

Fig. 1. Map of the study area indicating the fixed sampling site and mobile monitoring route. Traffic lights are presented as yellow circles, roundabout as blue circles, and mobile speed camera sites as red square.

Simultaneous measurements using the AE33 aethalometer and MA200 micro-aethalometer were performed in a measurement cycle of 80 h in order to compare the results from both instruments. The flows used were 5 L/min and 150 mL/min for AE33 and MA200, respectively. Both instruments sampled at 1 min intervals and had dryers to maintain a constant relative humidity (<35%). The obtained data was smoothed by a polynomial regression of grade 7, allowing the elimination of outliers and reduction of signal-to-noise.

Weather variables such as temperature, atmospheric pressure, relative humidity, wind speed, and wind direction were measured with a Vantage Pro2 weather station (Davis Instruments) near the fixed sampling site of the environmental BC measurements.

2.3. Determination of the absorption Ångström exponents

In general, it is assumed that the absorption Ångström exponent (AAE) for diesel emissions is close to 1 while that for biomass burning is close to 2 (Saturno et al., 2018). However, some variability in these values is usually observed. In the study area, the AAEs for biomass burning (AAE_{bb}) and fossil fuels (AAE_{ff}) were determined for all wavelength spectra measured from the mobile measurements as well as at the fixed monitoring site. For the AAE_{ff} characterization, measurements were taken at the city's transport terminal. The portable micro-aethalometer was operated at a distance of about 3 m from the emission points (exhaust of a diesel bus). After the engine of the vehicle was started, data was recorded at intervals of 1 min and a flow rate of 150 mL/min for 20 min. Data from a total of 5 buses was evaluated to take its variability into account. For determining AAE_{bb}, the controlled burning of small pieces of wood was carried out. The equipment was placed on a support at the height of 1 m above the floor. BC concentrations were recorded once the flaming stage began, and the recording was continued until the smoldering phase.

Due to the difference in the spectral dependence of aerosols resulting from the biomass burning (bb) and fossil fuel emissions (ff), it is possible to estimate the contribution of BC sources by calculating the AAE as per the model described by Sandradewi et al. (2008) using the blue channel ($\lambda = 470$ nm) and the infrared channel ($\lambda = 880$ nm) as follows:

$$AAE = \frac{\ln\left(\frac{b_{abs(470)}}{b_{abs(880)}}\right)}{\ln\left(\frac{470}{880}\right)} \quad (1)$$

where 470 and 880 nm are the wavelengths and $b_{abs(470)}$ and $b_{abs(880)}$ are the absorption coefficients at 470 and 880 nm, respectively.

2.4. Statistical analysis and special representation

In order to understand the behavior of the BC concentration and determine its contributing sources, an analysis of descriptive statistics by the sampling type (mobile and fixed) and K-means cluster analysis of the ambient sampling were performed. In the case of ambient monitoring, according to the similarity of information they provide, the AAEs were grouped into three groups: AAE corresponding to the vehicular traffic, biomass burning, and emissions from mixed sources (a mixture of the two sources indicated above). The analyses were performed using the IBM SPSS statistical software package (IBM SPSS Statistics version 22.0).

For representing the spatial distribution of BC concentration, results obtained in each sampling campaign were smoothed and converted into point vectors (shapefile) using the ArcGIS version 10.6 software. Subsequently, they were interpolated by the inverse distance weighting (IDW) method for each sampling campaign.

3. Results and discussions

3.1. Comparison of the results obtained from the AE33and MA200 instruments

AE33 has been widely used to determine not only BC concentrations, but also its your contribution to biomass burning and fossil fuel combustion sources, as an alternative to the methods based on chemical analysis of filter simples (Dumka et al., 2013; Becerril-Valle et al., 2017; Mousavi et al., 2019). Its usefulness the contribution of BC sources has been validated when compared with measurements of radiocarbon and levoglucosan source apportionment (Martinsson et al., 2017; Zotter et al., 2017), with Multiangle Absorption Photometer (MAAP) (Drinovec et al., 2015; Saturno et al., 2017) and even with previous versions of aethalometers obtaining a good relationship between them (Laing et al., 2020).

On the other hand, the microaethalometer has greater use in the spatial distribution of BC in urban areas (Hankey and Marshall, 2015), the evaluation of the personal exposure of BC (Madueño et al., 2019; Merritt et al., 2019) and recently the identification of biomass burning contributions using a MA200 due to supports to multiwavelengths setup (Stampfer et al., 2020).

The microathalometers are optical portable devices that link the attenuation rate (ΔATN) of a beam of light that passes through a filter spot to the concentration of black carbon. However, a comparison between the MA200 and AE51 was found to be non-linear due to some artefacts, the most important of which are the so-called shadowing effect linked with the increasing filter load and the multiple scattering of the filter fibers (Weingartner et al., 2003; Boniardi et al., 2019). The shadowing effect it is automatically corrected by the Dualspot© technology. This technology was available at MA200 and AE33.

In order to ensure the quality of the measurements, the BC concentrations obtained using the MA200 microaethalometer and the AE33 aethalometer were compared via the time series evaluation and linear regression (Fig. 2). As can be observed from the figure, in general, the results show good linear regression (Fig. 2b) and indicate similar behavior in the concentration-time series (Fig. 2a), yielding a linear regression coefficient of 0.9721 between the two measurements and an adjusted $R^2 = 0.933$. Thus, the results obtained from the two instruments can be related to $BC_{AE33} = 0.9721 \times BC_{MA200}$. An average difference of 9% in the concentrations between the two instruments is relatively small for the BC measurements since each instrument uses different absorption cross-sections, which, in turn, affects the conversion of light attenuation to BC mass concentrations.

Optical attenuation values measured by the aethalometer convert the BC mass concentration using the mass absorption cross-section (MAC) (Drinovec et al., 2015). MACs vary from one aethalometer model to another. For example, for calculating the BC concentration in the infrared wavelength region in the MA200, a MAC of 10.120 m^2/g is used, while, for AE33, a MAC of 7.77 m^2/g is used (the MACs were provided by the manufacturer). An adjusted R^2 linear coefficient of 0.933 indicates a good relationship between the measured concentrations obtained by the two aethalometers.

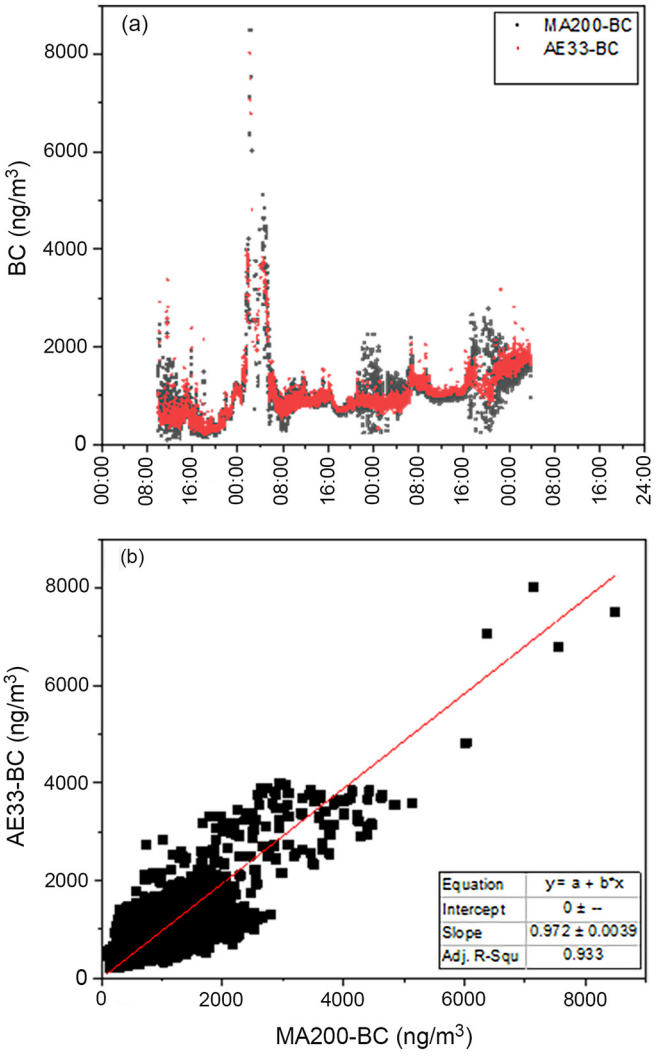

Fig. 2. (a) BC concentrations measured by the AE33 aethalometer (in red) and MA200 micro-aethalometer (in black), and (b) a plot of dispersion between the readings of the two instruments in ng/m^3.

The relative deviation between the two averaged concentrations of the instruments during the study period indicates that the microaethalometer underestimates the concentrations of BC at the 880 nm wavelength by 9.4%. This can be considered to be a relatively good result, since in the previous studies, such as those of Martins et al. (1998), Slowik et al. (2007) and Ajtai et al. (2011) a performance comparison between different aethalometers have shown differences of up to 40% for the measured concentrations.

3.2. Determination of AAEs for the local sources

Considering that the different chemical composition of fuels and vegetation around the world generate different BC emissions, the AAEs for diesel emissions (AAE_{ff}) and biomass burning (AAE_{bb}) in the study area were determined. These coefficients were determined under relatively controlled conditions, as mentioned previously in Section 2.3, with the portable microaethalometer (MA200) and the

results are presented in Table 1. Values for the biomass burning measurements show that AAE_{bb} varies over a wide range, with an average of 1.88 ± 0.49, which is close to 2, as expected. From the measurements on emissions from fossil fuels, AAE_{ff} values are close to 1, as expected, with an average of 0.97 ± 0.18. Harrison et al. (2013) reported similar results, with AAE_{ff} ranging between 0.8 and 1.1 and AAE_{bb} between 1.8 and 2.2. The higher variability in AAE_{bb} value is associated with factors such as the type of wood used, water content, and the phase of burning (i.e., flaming or smoldering). In addition, significant errors could be due to the absorption of finer aerosols at smaller wavelengths (Qiu et al., 2019).

In several studies, the values of AAE_{ff} obtained are mostly close to 1, as can be observed from Table 1. The variability in the AAE_{ff} values has been related to be due to factors such as the shape of the BC particle in the atmosphere, mixing state, aging, and coating. After emission, the AAE of the BC particles with compact structures can be coated by co-emitted organic compounds that may decrease the AAE_{ff} significantly, since the particle size increases that leads to a reduction of AAE_{ff} from 1.05 for fresh particles to 0.90 for aged aerosols (Liu et al., 2018a).

As can be seen from Table 1, the AAE_{ff} values found in this study are similar to those reported by Fuller et al. (2014) and Becerril-Valle et al. (2017), lower than those reported by Titos et al. (2017) and higher than the values reported by Zotter et al. (2017). The value obtained for AAE_{bb} (1.88) is close to the AAE found for residential coal combustion for home heating in Beijing, China (1.87 ± 0.64) (Liu et al., 2018b). It is larger than the values obtained in a smog chamber for fresh and photochemically aged emissions of different types of wood (1.63 ± 0.32) (Saleh et al., 2013) and also for other measurements (Becerril-Valle et al., 2017; Zotter et al., 2017).

Although the AAE values presented in this section provide particular data for a specific source (fossil fuel and biomass burning) in a complex urban environment, this condition of contribution from a single BC source is, in general not observed, but a mixture of variable contributions of fossil fuel and biomass burning emissions.

3.3. Spatial variability of BC concentration

Results obtained from the data analysis of the mobile sampling carried out in this study, corresponding to the BC concentration measured at the infrared wavelength (880 nm) and a MAC of 10.12 m^2/g, have been presented in Table 2. The average value of BC concentration and its standard deviation obtained from all BC samples is found to be a high value of 16.1 ± 16.5 $\mu g/m^3$. It is important to mention here that the exposure of the population that spends a significant amount of time in public transportation is related to this high BC value. As expected, and will also be discussed in the following paragraphs, the variability of BC concentration is due to various spatial factors such as traffic density, terrain topology, as well as the proximity of emission sources (Van Poppel et al., 2013; Li et al., 2015).

The spatial distribution of BC concentration from all the measurements recorded during the study period is shown in Fig. 3a. The different colors represent a specific average concentration for the region. High concentrations of BC (>20 $\mu g/m^3$) along the route were recorded in the southern part of the city, downwind of the urban center. This area is characterized by a larger number of traffic intersections and speed detection cameras in comparison to the north of the city. This provides points with notable vehicular congestion and low vehicle speed that led to higher levels of BC than in the other parts of the study area. On the other hand, lower levels of BC were identified in the north of the city, which has an average vehicle speed of 80 km/h and thus is a fast-moving route with little traffic. This facilitates vehicle distancing and ease of dispersion of the emissions. The speed limit in the southern part of the city is much lower at 30 km/h, which increases BC emission and concentration.

The observations described above are a general feature found from other studies as well Ham et al. (2017) have observed that intersections are the main contributing factor to the high concentration of BC, since vehicle congestion accompanied by the stop and go effect of vehicles can result in higher levels of incomplete combustion. Similarly, highways and main roads were observed to have a high concentration of BC due to traffic congestion in yet another study (Krecl et al., 2014). In addition, a higher BC concentration is usually present near the traffic intersections as compared to a street curb, a street canyon or an urban background, as has been already shown by Goel and Kumar (2014).

The proportion of heavy diesel vehicles and weather variables certainly influences the BC concentration. In Barranquilla, the vehicle fleet in 2018 consisted of 10% of diesel-fueled vehicles. However, a high value of 35% of the total fuel was sold during the same year, which despite being a small proportion of the vehicle fleet, significantly favors a higher BC concentration (Targino et al., 2016). Ježek et al. (2015), in their study on emission factors, concluded that only 25% of diesel-fueled vehicles contributed about 63% to the BC emissions. On the other hand, meteorological variables measured on the roads have been observed to show little influence on mobile BC concentration measurements, which are mostly affected by the continually changing traffic environment and near-surface weather conditions (Dons et al., 2012).

In order to understand the pattern of BC emission in the study area, the spatial distribution was separated into two datasets, working days (Fig. 3b) and non-working days (Fig. 3c) and average BC concentration values of 17.8 ± 17.3 $\mu g/m^3$ and 7.10 ± 5.49 $\mu g/m^3$ respectively, were obtained for the two sets. Both figures highlight the effects of vehicular traffic, showing a 2.5 times higher concentration of BC on working days as compared to the non-working days.

Table 1
Comparison of AAE_{ff} and AAE_{bb} obtained in this study with those from different studies.

AEE_{ff}	AAE_{bb}	Wavelengths used	Reference
0.97	1.88	470 and 880 nm	This study
1.05 fresh BC	N/R	N/R	Liu et al., 2018b
0.90	1.75	470 and 880 nm	Zotter et al. (2017)
1.1	2.0	370 and 970 nm	Titos et al. (2017)
0.97–1.12	1.63–1.74	470 and 950 nm	Becerril-Valle et al. (2017)
1.0	1.8	407 and 850 nm	Massabò et al. (2015))
N/A	2.5	370 and 950 nm	Martinsson et al. (2015)
0.96	NR	370 and 880 nm	Fuller et al. (2014)
0.8–1.1	1.8–2.2	370 and 880 nm	Harrison et al. (2013)
N/R	1.38 for fresh oak 1.48 for the fresh fewin pine 2.15 for fresh blueberry	370 and 950 nm	Saleh et al. (2013)
1.1	1.86	470 and 950 nm	Sandradewi et al. (2008)
1.0	2.5	UV- IR	Kirchstetter et al. (2004)

Note: N/R = No report.

Table 2
Descriptive statistics for BC concentrations and meteorological conditions.

Parameters	Mobile monitoring				Ambient			
	Mean	Standard deviation	Min	Max	Mean	Standard deviation	Min	Max
BC (μg/m^3)	16.1	16.5	0.66	140.4	1.04	1.03	0.16	10.27
AAE	0.91	0.15	0.48	1.40	1.22	0.12	0.92	2.33
Air temperature (°C)	29.34	1.23	26.6	31.4	28.50	1.47	24.93	32.82
Relative humidity (%)	77.85	4.24	69.0	86.0	85.22	6.33	63.83	96.00
Wind speed (m/s)	4.28	1.77	0.4	9.8	2.43	1.78	0.00	7.43
Wind direction (°)	86	60	23	293	94	45	11	291
N° of samples	232				1393			

On comparison of our results with other investigations, it was observed that in Bogotá, Colombia, BC concentration was reported to have an average value of 33.8 μg/m^3 during the working days and 19.8 μg/m^3 during the weekends (Franco et al., 2016), while, in São Paulo, Brazil, the BC concentration was between 8.5 and 10 times higher on working days as compared to non-working days (Targino et al., 2018). The BC concentration in both cases is attributable to the different vehicular traffic patterns and the configuration of roads (cycle paths). In São Paulo, for example, the vehicle fleet is 7.8 million, corresponding to 83.5% cars, 13.4% motorcycles, 1.1% buses, and 2.0% trucks. The study area evaluated by Targino et al. (2018), was influenced by a high number of motor vehicles (5136 vehicles/h), of which 4.9% were heavy-duty diesel vehicles. In Bogotá, vehicle flow in the study sections located along the main roads was between 2713 and 12,838 vehicles/h (Franco et al., 2016).

The AAE results for the spatial distribution in this study indicate that it remains quite constant with an average value of 0.90 ± 0.15 throughout the experiments. This coefficient is similar to AAE_{ff} reported in the source measurements having an average value of 0.97 ± 0.18. This confirms that traffic is the main source of BC in the mobile monitoring study. The AAE evaluation was done to estimate the possible contributions from biomass burning sources, since some industries located along with the route use wood burning in their boilers. However, this influence was found to be insignificant in this study.

The comparison of the BC concentration values measured in this study with those obtained from other studies is given in Table 3. Although the use of mobile platforms, measuring equipment, and study objectives are different between the investigations, all the studies provide the key information on the use of mobile monitoring in urban environments. From a comparison of the results of this study with those obtained in other cities, it is seen that the BC levels measured in this study in Barranquilla were higher than those found in Shanghai (Li et al., 2015; Lei et al., 2017; Liu et al., 2019a; Liu et al., 2019b), Brisbane (Williams and Knibbs, 2016), Londrina (Targino et al., 2016), Minneapolis (Hankey and Marshall, 2015), Stockholm (Krecl et al., 2014), Beckley (Jarjour et al., 2013), Helsinki, Rotterdam, and Thessaloniki (Okokon et al., 2017) and lower than those reported in Barcelona (de Nazelle et al., 2012), and Bogotá (Franco et al., 2016). It is important to emphasize that Barranquilla is a much smaller urban area than most of the cities listed in Table 3. The old age of the urban bus fleet and the lack of a vehicle inspection program certainly contributes to the significantly higher values of BC concentration measured in Barranquilla.

3.4. Measurements of ambient BC concentration

A time series of the daily mean BC concentrations measured at the infrared wavelength (880 nm) and AAE values obtained from them during the study period for the evaluation of ambient BC is shown in Fig. 4. Hourly BC levels up to 10.3 and 9.26 μg/m^3 were observed and with the corresponding AAEs of 1.06 and 1.12, respectively. In this way, as expected for the urban areas, the highest concentration was associated with vehicular traffic emissions. On the other hand, several events with higher AAEs were observed (on 6th, 18th, and 20th May and 15th, 16th, 26th, and 30th June) and were associated with biomass burning emissions around the study area. The highest AAE values were between 1.44 and 2.33. During these days, as confirmed by remote sensing tools, a series of biomass burning plumes were recorded in the surroundings of the city of Barranquilla due to the mangrove burns made in the Vía Isla Salamanca Natural Park.

Variation of the burning points is mainly associated with climatic conditions and the intensity of the activities that generate biomass burning. Therefore, their contribution during the study period is not constant. In dry periods there is a greater number of burning points, which are associated with a greater emission of BC from this source.

The diel variability of BC concentration and AAE are presented in Fig. 5a and b, respectively. Three peaks corresponding to higher BC concentration are evident: in the morning (06:00–09:00 h) having a concentration of 2.14 μg/m^3; in the afternoon, around 14:00 having a concentration of 1.07 μg/m^3 and during the night (18:00–20:00 h) having a maximum value of 1.09 μg/m^3. On the other hand, the diel variability of AAE, which relates the BC concentration with vehicular traffic emissions, coinciding, in turn, with the hours of the highest vehicular traffic, is seen to have constant values <1.20 in the same hours. In addition, the location of the sampling site, downwind of a road having high vehicular traffic, is a determining factor in this pattern of BC concentration (Taheri et al., 2019).

The daytime variations of BC concentration during the working days and non-working days show a trend similar to BC concentration obtained from measurements throughout the days and nights and on both working as well as non-working days (all data), with pronounced peaks seen during the morning (6:00–9:00 h) and at night (18:00–20:00 h). The concentration of BC recorded on working days correspond to 1.16 ± 0.48 μg/m^3 while that recorded on non-working days correspond to 0.78 ± 0.33 μg/m^3. Thus, the BC concentration on working days is 1.5 times higher as compared to the non-working days.

In this study, the behavior of BC concentration coincides with the profiles of an urban center, due to the contribution of vehicular traffic and the proximity of the sampling site to the main roads. Similar patterns of BC concentration were found in the suburban and urban areas in the United Kingdom (Singh et al., 2018), in Nanjing, China (Xiao et al., 2020), and Madurai, India (Bhaskar et al., 2018) and are generally attributed to the atmospheric boundary layer height, weather conditions, and local anthropogenic emissions (Ribeiro et al., 2010, 2013; Oliveira et al., 2012, 2014, 2017; Quispe et al., 2012; Ehrenbring et al., 2019).

In order to observe the pattern of BC concentration according to its sources, three categories were identified and classified according to a K-means cluster analysis, using the AAE values as a grouping criterion. The first cluster, related to the BC resulting from fossil fuel emissions (Fig. 5b and Table 4), has AAE in the range of 0.92 to 1.23 and a mean BC concentration of 1.18 ± 1.15 μg/m^3. The second cluster, related to the biomass burning (Fig. 5b and Table 4), has AAE values between 1.44 and 2.33, with an average BC concentration of 0.81 ± 1.56 μg/m^3, slightly lower than the previous one. Finally, a category composed of a mixture of the two sources (fossil fuel emissions and biomass burning)

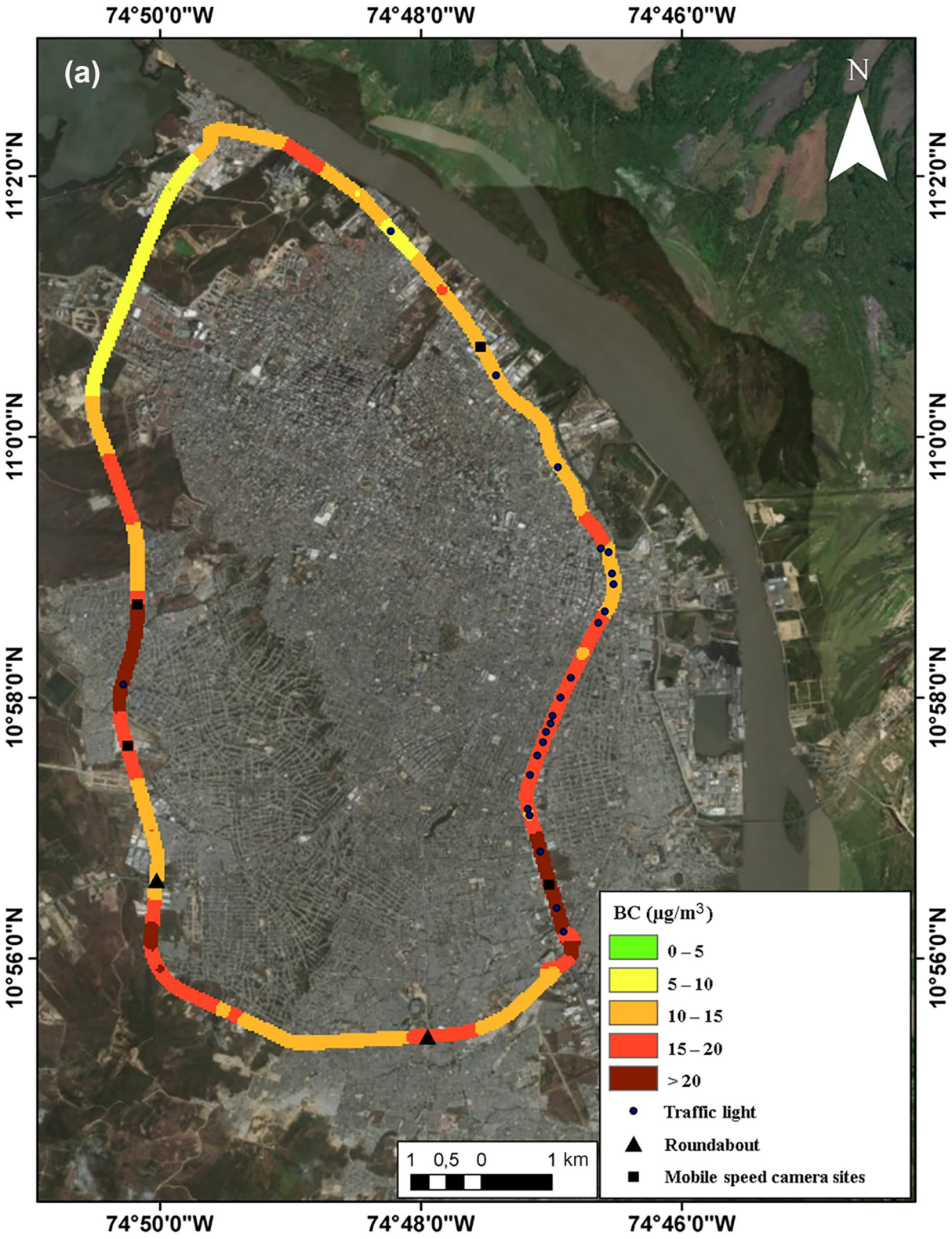

Fig. 3. Spatial distribution of aggregated median BC concentrations for (a) all sampling sessions, (b) working days with $n = 11$ routes, and (c) non-working days with $n = 2$ routes.

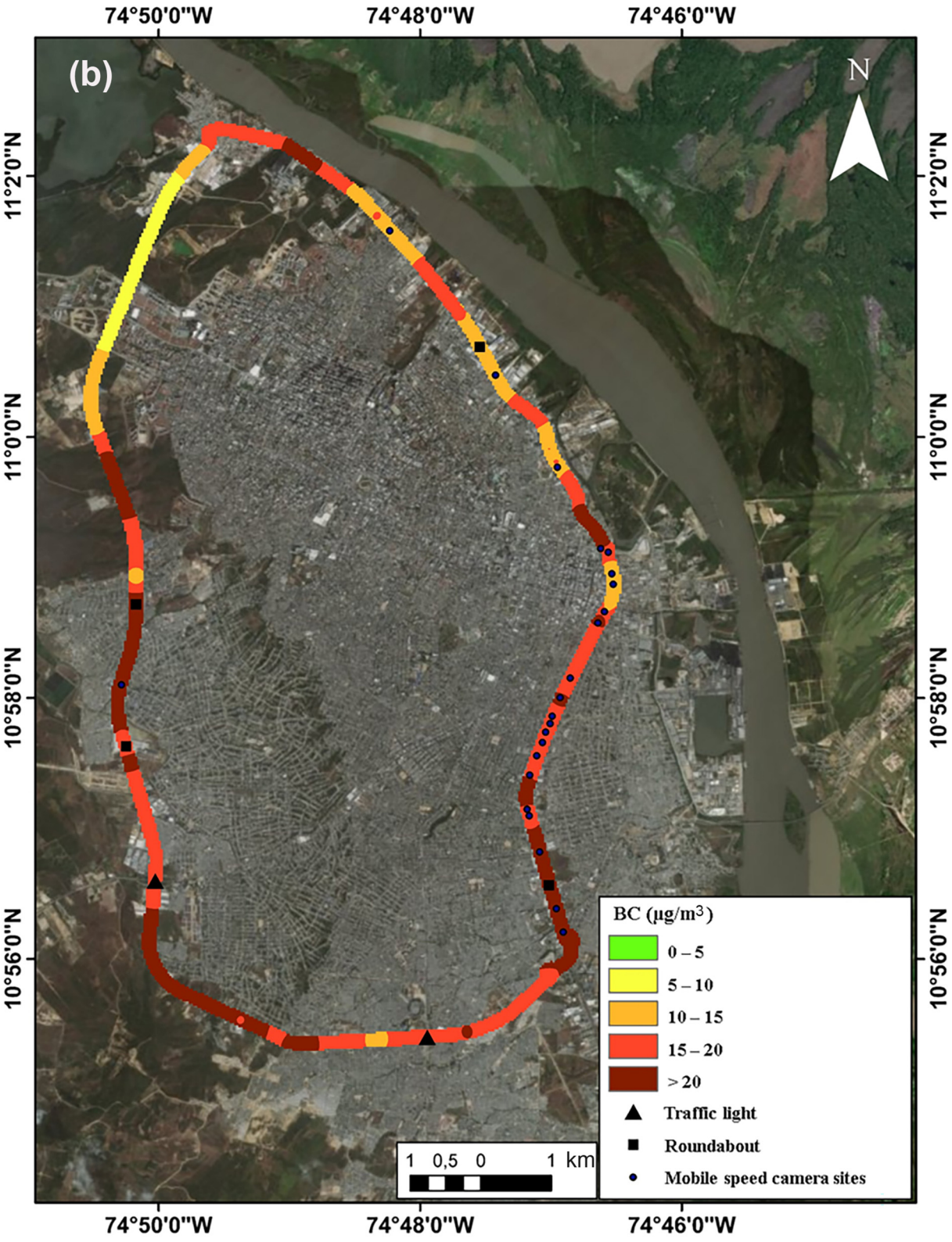

Fig. 3 (*continued*).

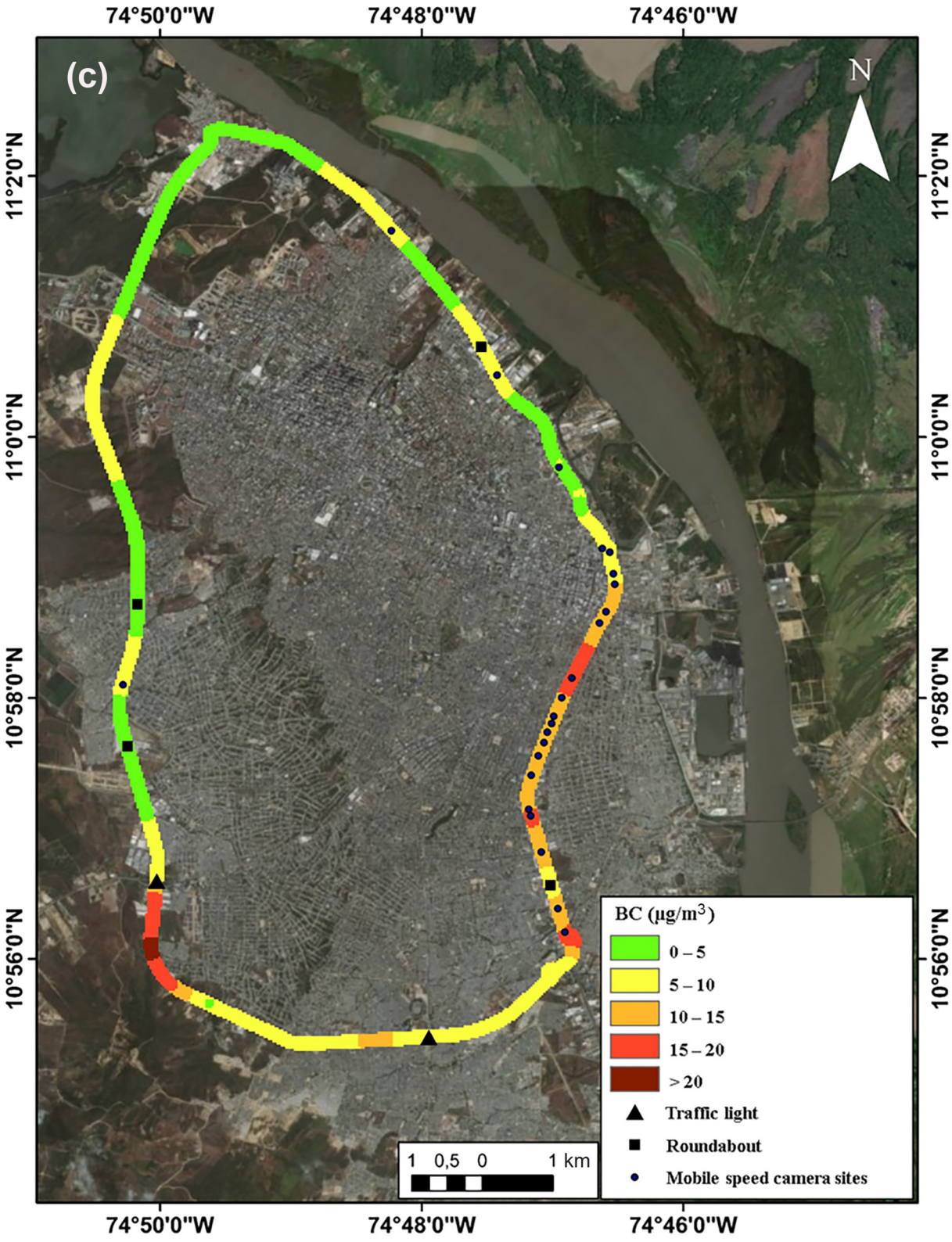

Fig. 3 (*continued*).

Table 3
Comparisons of BC concentrations in urban areas, obtained for mobile monitoring, from different studies.

City	Study year	BC ± SD (μg/m^3)	Reference
Barranquilla, Colombia	2018	16.1 ± 16.54	This study
São Paulo, Brazil	2017	8.5 ± 8.4 Weekday (B) 5.2 ± 13.9 Weekday	Targino et al. (2018)
Macau, China	2016	4.0 ± 2.6 (morning) 3.1 ± 1.9 (afternoon)	Liu et al. (2019a)
Shanghai, China	2016	10.8 ± 3.5 (C)	Liu et al. (2019b)
Shanghai, China	2015	11.8 ± 9.8 (C)	Lei et al. (2017)
Brisbane, Australia	2015	4.4 ± 7.3 (OWC)	Williams and Knibbs (2016)
Londrina, Brazil	2015	6.35 ± 20.0 (morning) 5.10 ± 14.7 (afternoon) (B)	Targino et al. (2016)
Shanghai, China	2014	7.28 ± 1.63 (Bs) 9.43 ± 1.70 (S) 8.62 ± 2.57 (T)	Li et al. (2015)
Bogota, Colombia	2013	25.6 ± 39.2 (B)	Franco et al. (2016)
Minneapolis, USA	2012	2.5 ± 1.4 (morning) 0.7 ± 1.6 (afternoon) (B)	Hankey and Marshall (2015)
Stockholm, Sweden	2011	2.4 ± 3.6 (T)	Krecl et al., 2014
Berkeley, USA	2011	1.76 ± 2.58 low traffic (B) 2.06 ± 3.23 high traffic (B)	Jarjour et al. (2013)
Helsinki (urban)	2011	7.8 ± 4.3 (OWC)	Okokon et al. (2017)
Rotterdam (urban)	2011	6.4 ± 3.3 (OWC)	
Thessaloniki (urban)	2011	10.9 ± 9.9 (OWC)	
Barcelona, Spain	2009	16.7 (C)	de Nazelle et al. (2012)

Note: Bs (bus), S (subway), T (Taxi), C (cars), OWC (open windows car), B (bicycle).

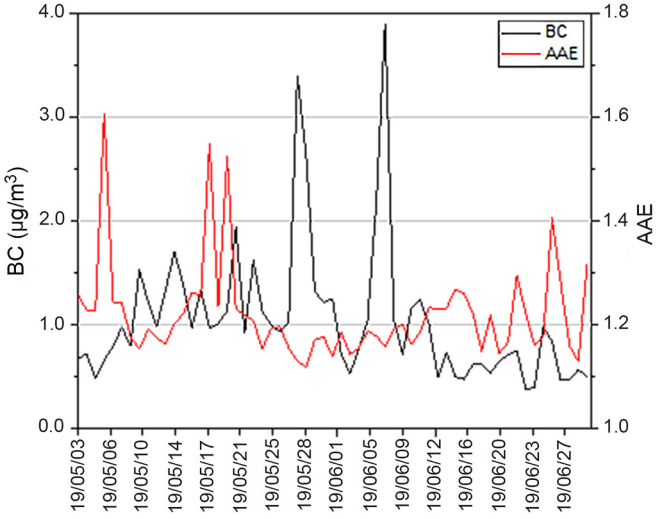

Fig. 4. Daily average time series for ambient BC concentrations and AAE during the study period.

(Fig. 5b and Table 4), which has been called mixed sources, has AAE in the range of 1.23 to 1.44 and an average BC concentration of 0.78 ± 1.29 μg/m^3. Therefore, the concentration of BC recorded for the ambient monitoring corresponds to 66% of fossil fuel emissions, 6% of burning biomass, and 28% of mixed sources.

The results indicate that AAE_{ff} and AAE_{mixed} have a limited magnitude of 1.15 ± 0.05 and 1.29 ± 0.05, respectively, while AAE_{bb} has a larger magnitude of 1.56 ± 0.14. Becerril-Valle et al. (2017) observed similar AAE profiles in Madrid, Spain, with a relatively flat trend in an urban background (1.05 ± 0.05 in spring and 1.07 ± 0.06 in autumn) and in the urban center (1.16 ± 0.08 in spring and 1.07 ± 0.07 in autumn), while in Paris, France, AAE values of 1.02 ± 0.04 (summer) during peak morning traffic and 1.08 ± 0.04 during the evening/night periods were reported in another study (Favez et al., 2009). In both cases, the seasons are characterized by the predominance of vehicular traffic as a significant source.

The behavior of BC concentration for the biomass burning category (Fig. 5a) is strongly marked by peak values in the morning and at night, although it is in an urban area with the influence of vehicular traffic. The biomass burning events recorded during the study originate from burning activities coming from the northeast and east of the city. A natural mangrove reserve is located in this area, in which illegal biomass burning occurs to obtain agricultural areas and for charcoal production.

The continuous measurements of ambient BC concentration in this study show an average value of 1.04 ± 1.03 μg/m^3 (Table 2). According to measurements carried out in other cities, the results are lower than those reported in urban areas such as Nanjing, China (1.328 ± 1.12 μg/m^3) (Jing et al., 2019), Istanbul, Turkey (13 ± 4 μg/m^3) (Ozdemir et al., 2014), Milan, Italy (1.92 ± 0.35 μg/m^3) (Mousavi et al., 2019), Trivandrum, Kerala (3.51 ± 1.64 μg/m^3) (Rajeevan et al., 2019), Los Angeles, California (2.89 ± 0.84 μg/m^3) (Shirmohammadi et al., 2017), and Rio de Janeiro, Brazil (1.6 ± 1–3.3 ± 1.7 μg/m^3) (Godoy et al., 2009).

Although these are only the initial results of a continuous monitoring carried out in the city of Barranquilla, it is evident that the rapid dispersion of BC occurs as a result of emissions from mobile sources (average value of 16.17 μg/m^3) until reaching the fixed monitoring point (average value of 1.04 μg/m^3). The study area is located in a coastal area, characterized by high wind speeds influenced by sea and land breezes, who play a significant role favoring contaminant dispersion processes and consequently improving the air quality. These results contrast with those reported by Aruna et al. (2013) and Kumar et al. (2020) where stations located in the coastal region of southern India report low concentrations of BC compared to urban areas and semi-urban.

There are some limiting aspects in BC mobile monitoring that can influence the representativeness of the results, such as the collection of mobile data carried out in limited periods of time, the number of experiments, the different mobile platforms and the routes traced. However,

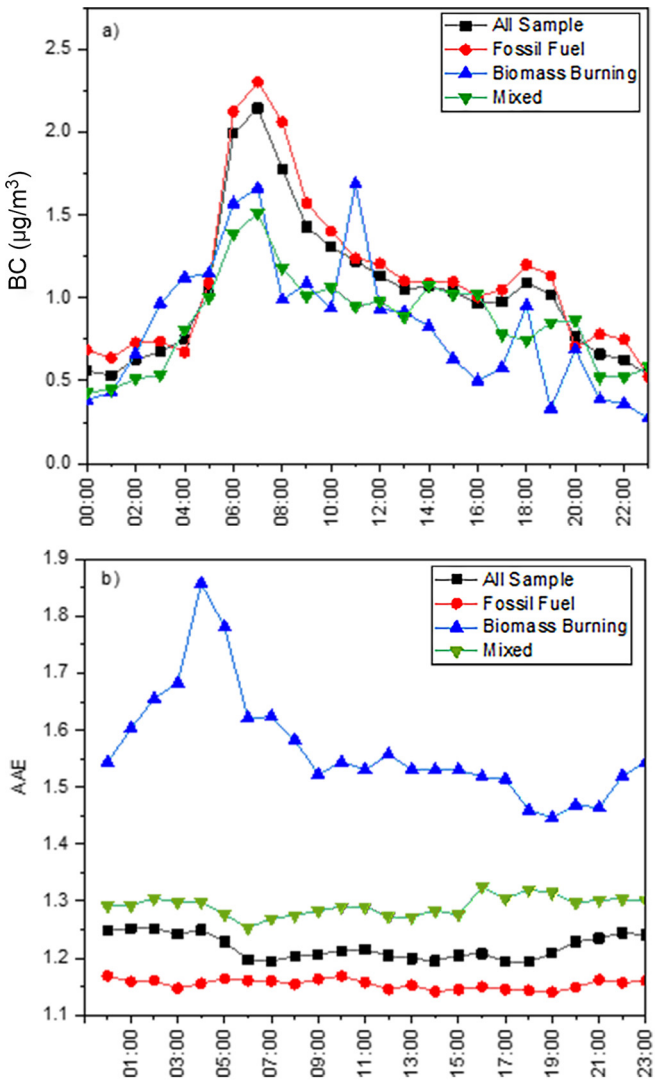

Fig. 5. (a) Daily variation of black carbon concentration (μg/m^3), and (b) AAE in the categories general, fossil fuel, mixed and biomass burning.

Table 4
Source apportionment of BC.

	Fossil fuel		Mixed		Biomass burning	
	BC (μg/m^3)	AAE	BC (μg/m^3)	AAE	BC (μg/m^3)	AAE
Mean	1.18	1.15	0.78	1.29	0.81	1.56
Standard deviation	1.16	0.05	0.65	0.05	0.59	0.14
Min	0.16	0.92	0.17	1.23	0.24	1.44
Max	10.27	1.23	5.38	1.44	3.28	2.33
N° of samples	911		396		78	

this study allows understanding of the BC formation and spatial distribution processes.

4. Conclusions

BC concentration was evaluated through ambient monitoring and mobile measurements in an urban area of the Colombian Caribbean. The average concentration of ambient BC was found to be 1.04 ± 1.03 μg/m^3. As described in the results, the concentration implied a strong association with local emission sources. The hourly profiles of BC and AAE indicate that the emissions originate from fossil fuels and consequently, are associated with vehicular traffic, the predominant source of BC. This source was observed to be the primary source in 66% of the evaluated period, which is a characteristic of urban areas. However, during the same period, the influence of 6% of data frequency was observed to be due to biomass burning, registered mainly in the park via Isla Salamanca. The remaining 28% of the data was associated with mixed sources, consisting of the contribution of both vehicular traffic and biomass burning.

Results found in the ambient BC and AAE associate biomass burning emissions around the study area. Therefore, extending the sampling period will allow studying the temporal variability of the pollutant, as well as the optical properties and its sources of BC emission. Additionally, the use of digital platforms is suggested to identify the sources of fires that allow evidence of the impact of forest burns in the region in the company of air mass trajectory models.

The spatial variability of BC concentration was associated with local traffic, showing an average concentration of 16.1 ± 16.5 μg/m^3. Hotspots with high BC concentration were registered near the urban center, in areas with high vehicular congestion produced by different road infrastructures and transport such as road intersections, speed reducers, and speed limit control of the road.

In this study, it is shown that as compared to the AE33 aethalometer, validated by the United States Environmental Protection Agency (US EPA), the MA200 portable micro-aethalometer can also be used to determine the BC concentration. This instrument has been used to determine not only BC concentrations, but also its your contribution to biomass burning and fossil fuel combustion sources from the AAE calculation. Its low price and ease of use make it an attractive instrument for BC.

Finally, as a suggestion, the use of both methods (mobile and fixed) for BC measurement in complex urban centers is recommended so that the spatial-temporal variations of BC concentration can be highlighted. These results will contribute to the construction of policies and strategies that help to reduce BC concentration in the city and consequently its effects on population health and climate change.

Supplementary data to this article can be found online at https://doi.org/10.1016/j.gsf.2021.101149.

Declaration of competing interest

The authors declare that they have no known competing financial interests or personal relationships that could have appeared to influence the work reported in this paper.

Acknowledgements

This research was supported by the Department of Civil and Environmental of the Universidad de la Costa, the Center for Environmental Technology Research (Centro de Investigación de Tecnologías Ambientales – CITA), the Environmental Management and Sustainability Research Group (Grupo de Investigación de Gestión y Sostenibilidad Ambiental – GESSA) and with partial financial support from Colciencias, Colombia (Project 141180764164, Contract 815-2018).

References

US EPA – United States Environmental Protection Agency, 2012. Report to Congress on Black Carbon, EPA-450/R-12-001. Environmental Protection Agency, Office of Air and Radiation, Washington (48 pp).

de Nazelle, A., Fruin, S., Westerdahl, D., Martinez, D., Ripoll, A., Kubesch, N., Nieuwenhuijsen, M., 2012. A travel mode comparison of commuters' exposures to air pollutants in Barcelona. Atmos. Environ. 59, 151–159.

Dons, E., Panis, L.I., Van Poppel, M., Theunis, J., Wets, G., 2012. Personal exposure to Black Carbon in transport microenvironments. Atmos. Environ. 55, 392–398.

Favez, O., Cachier, H., Sciare, J., Sarda-Estève, R., Martinon, L., 2009. Evidence for a significant contribution of wood burning aerosols to $PM_{2.5}$ during the winter season in Paris, France. Atmos. Environ. 43 (22–23), 3640–3644.

Schneider, I.L., Teixeira, E.C., Agudelo-Castañeda, D.M., Silva e Silva, G., Balzaretti, N., Braga, M.F., Oliveira, L.F.S., 2016. FTIR analysis and evaluation of carcinogenic and mutagenic risks of nitro-polycyclic aromatic hydrocarbons in $PM_{1.0}$. Sci. Total Environ. 541, 1151–1160.

Agudelo-Castañeda, D.M., Teixeira, E.C., Schneider, I.L., Pereira, F.N., Oliveira, M.L.S., Taffarel, S.R., Sehn, J.L., Ramos, C.G., Silva, L.F.O., 2016. Potential utilization for the evaluation of particulate and gaseous pollutants at an urban site near a major highway. Sci. Total Environ. 543 (A), 161–170.

Agudelo-Castañeda, D.M., Teixeira, E.C., Schneider, I.L., Lara, S.R., Silva, L.F.O., 2017. Exposure to polycyclic aromatic hydrocarbons in atmospheric PM1.0 of urban environments: Carcinogenic and mutagenic respiratory health risk by age groups. Environ. Pollut. 224, 158–170.

Ajtai, T., Filep, Á., Utry, N., Schnaiter, M., Linke, C., Bozóki, Z., Szabó, G., Leisner, T., 2011. Inter-comparison of optical absorption coefficients of atmospheric aerosols determined by a multi-wavelength photoacoustic spectrometer and an Aethalometer under sub-urban wintry conditions. J. Aerosol Sci. 42 (12), 859–866.

Artaxo, P., Rizzo, L.V., Brito, J.F., Barbosa, H.M.J., Arana, A., Sena, E.T., Cirino, G.G., Bastos, W., Martin, S.T., Andreae, M.O., 2013. Atmospheric aerosols in Amazonia and land use change: from natural biogenic to biomass burning conditions. Faraday Discuss. 165, 203–235.

Aruna, K., Kumar, T.V.L., Rao, D.N., Murthy, B.V.K., Babu, S.S., Moorthy, K.K., 2013. Black carbon aerosols in a tropical semi-urban coastal environment: effects of boundary layer dynamics and long range transport. J. Atmos. Sol.-Terr. Phy. 104, 116–125.

Becerril-Valle, M., Coz, E., Prévôt, A.S.H., Močnik, G., Pandis, S.N., Sánchez de la Campa, A.M., Alastuey, A., Díaz, E., Pérez, R.M., Artíñano, B., 2017. Characterization of atmospheric black carbon and co-pollutants in urban and rural areas of Spain. Atmos. Environ. 169, 36–53.

Bergstrom, R.W., Russell, P.B., Hignett, P., 2002. Wavelength dependence of the absorption of black carbon particles: predictions and results from the TARFOX experiment and implications for the aerosol single scattering albedo. J. Atmos. Sci. 59, 567–577.

Bhaskar, B.V., Rajeshkumar, R.M., Muthuchelian, K., Ramachandran, S., 2018. Spatial, temporal and source study of black carbon in the atmospheric aerosols over different altitude regions in Southern India. J. Atmos. Sol.-Terr. Phy. 179, 416–424.

Bond, T.C., Bergstrom, R.W., 2006. Light absorption by carbonaceous particles: an investigative review. Aerosol Sci. Technol. 40 (1), 27–67.

Bond, T.C., Doherty, S.J., Fahey, D.W., Forster, P.M., Berntsen, T., DeAngelo, B.J., Flanner, M.G., Ghan, S., Kärcher, B., Koch, D., Kinne, S., Kondo, Y., Quinn, P.K., Sarofim, M.C., Schultz, M.G., Schulz, M., Venkataraman, C., Zhang, H., Zhang, S., Bellouin, N., Guttikunda, S.K., Hopke, P.K., Jacobson, M.Z., Kaiser, J.W., Klimont, Z., Lohmann, U., Schwarz, J.P., Shindell, D., Storelvmo, T., Waren, S.G., Zender, C.S., 2013. Bounding the role of black carbon in the climate system: a scientific assessment. J. Geophys. Res. Atmos. 118 (11), 5380–5552.

Boniardi, L., Dons, E., Campo, L., Van Poppel, M., Panis, L.I., Fustinoni, S., 2019. Annual, seasonal, and morning rush hour Land Use Regression models for black carbon in a school catchment area of Milan, Italy. Environ. Res. 176, 108520.

Boucher, O., Randall, D., Artaxo, P., Bretherton, C., Feingold, G., Forster, P., Kerminen, V.-M., Kondo, Y., Liao, H., Lohmann, U., Rasch, P., Satheesh, S.K., Sherwood, S., Stevens, B., Zhang, X.-Y., 2013. Clouds and Aerosols. In: Climate Change 2013: The Physical Science Basis. Contribution of Working Group I to the Fifth Assessment Report of the Intergovernmental Panel on Climate Change. New York, NY, USA. pp. 571–658.

Brito, J., Rizzo, L.V., Herckes, P., Vasconcellos, P.C., Caumo, S.E.S., Fornaro, A., Ynoue, R.Y., Artaxo, P., Andrade, M.F., 2013. Physical–chemical characterisation of the particulate matter inside two road tunnels in the São Paulo Metropolitan Area. Atmos. Chem. Phys. 13 (24), 12199–12213.

Coen, M.C., Weingartner, E., Apituley, A., Ceburnis, D., Fierz-Schmidhauser, R., Flentje, H., Henzing, J.S., Jennings, S.G., Moerman, M., Petzold, A., Schmid, O., Baltensperger, U., 2010. Minimizing light absorption measurement artifacts of the Aethalometer: evaluation of five correction algorithms. Atmos. Meas. Tech. 3 (2), 457–474.

Rizzo, L.V., Correia, A.L., Artaxo, P., Procópio, A.S., Andreae, M.O., 2011. Physics spectral dependence of aerosol light absorption over the Amazon Basin. Atmos. Chem. Phys. 11 (17), 8899–8912.

Drinovec, L., Močnik, G., Zotter, P., Prévôt, A.S.H., Ruckstuhl, C., Coz, E., Rupakheti, M., Sciare, J., Müller, T., Wiedensohler, A., Hansen, A.D.A., 2015. The "dual-spot" Aethalometer: an improved measurement of aerosol black carbon with real-time loading compensation. Atmos. Meas. Tech. 8 (5), 1965–1979.

Duarte, A.L., DaBoit, K., Oliveira, M.L.S., Teixeira, E.C., Schneider, I.L., Silva, L.F.O., 2019. Hazardous elements and amorphous nanoparticles in historical estuary coal mining area. Geosci. Front. 10 (3), 927–939.

Dumka, U.C., Manchanda, R.K., Sinha, P.R., Sreenivasan, S., Moorthy, K.K., Babu, S.S., 2013. Temporal variability and radiative impact of black carbon aerosol over tropical urban station Hyderabad. J. Atmos. Sol.-Terr. Phy. 105–106, 81–90.

Ehrenbring, H.Z., de Medeiros Quinino, U.C., Oliveira, L.F.S., Tutikian, B.F., 2019. Experimental method for investigating the impact of the addition of polymer fibers on drying shrinkage and cracking of concretes. Struct. Concr. 20 (3), 1064–1075.

Evans, M., Kholod, N., Kuklinski, T., Denysenko, A., Smith, S.J., Staniszewski, A., Hao, W.M., Liu, L., Bond, T.M., 2017. Black carbon emissions in Russia: a critical review. Atmos. Environ. 163, 9–21.

Franco, J.F., Segura, J.F., Mura, I., 2016. Air pollution alongside bike-paths in Bogotá-Colombia. Front. Environ. Sci. 4, 77.

Fuller, G.W., Tremper, A.H., Baker, T.D., Yttri, K.E., Butterfield, D., 2014. Contribution of wood burning to PM_{10} in London. Atmos. Environ. 87, 87–94.

Godoy, M.L.D.P., Godoy, J.M., Roldão, L.A., Soluri, D.S., Donagemma, R.A., 2009. Coarse and fine aerosol source apportionment in Rio de Janeiro, Brazil. Atmos. Environ. 43 (14), 2366–2374.

Goel, A., Kumar, P., 2014. A review of fundamental drivers governing the emissions, dispersion and exposure to vehicle-emitted nanoparticles at signalised traffic intersections. Atmos. Environ. 97, 316–331.

Gong, T., Sun, Z., Zhang, X., Zhang, Y., Wang, S., Han, L., Zhao, D., Ding, D., Zheng, C., 2019. Associations of black carbon and $PM_{2.5}$ with daily cardiovascular mortality in Beijing, China. Atmos. Environ. 214, 116876.

Ham, W., Vijayan, A., Schulte, N., Herner, J.D., 2017. Commuter exposure to $PM_{2.5}$, BC, and UFP in six common transport microenvironments in Sacramento, California. Atmos. Environ. 167, 335–345.

Hankey, S., Marshall, J.D., 2015. On-bicycle exposure to particulate air pollution: particle number, black carbon, $PM_{2.5}$ and particle size. Atmos. Environ. 122, 65–73.

Harrison, R.M., Beddows, D.C.S., Jones, A.M., Calvo, A., Alves, C., Pio, C., 2013. An evaluation of some issues regarding the use of aethalometers to measure woodsmoke concentrations. Atmos. Environ. 80, 540–548.

Jarjour, S., Jerrett, M., Westerdahl, D., de Nazelle, A., Hanning, C., Daly, L., Lipsitt, J., Balmes, J., 2013. Cyclist route choice , traffic-related air pollution , and lung function : a scripted exposure study. Environ. Health 12, 14.

Ježek, I., Katrašnik, T., Westerdahl, D., Močnik, G., 2015. Black carbon, particle number concentration and nitrogen oxide emission factors of random in-use vehicles measured with the on-road chasing method. Atmos. Chem. Phys. 15 (19), 11011–11026.

Jing, A., Zhu, B., Wang, H., Yu, X., An, J., Kang, H., 2019. Source apportionment of black carbon in different seasons in the northern suburb of Nanjing, China. Atmos. Environ. 201, 190–200.

Kirchstetter, T.W., Novakov, T., Hobbs, P.V., 2004. Evidence that the spectral dependence of light absorption by aerosols is affected by organic carbon. J. Geophys. Res. 109 (D21), D21208.

Krecl, P., Johansson, C., Ström, J., Lövenheim, B., Gallet, J., 2014. A feasibility study of mapping light-absorbing carbon using a taxi fleet as a mobile platform. Tellus B 66 (1), 23533.

Kumar, R.R., Soni, V.K., Jain, M.K., 2020. Evaluation of spatial and temporal heterogeneity of black carbon aerosol mass concentration over India using three year measurements from IMD BC observation network. Sci. Total Environ. 723, 138060.

Laing, J.R., Jaffe, D.A., Sedlacek, A.J., 2020. Comparison of filter-based absorption measurements of biomass burning aerosol and background aerosol at the Mt. Bachelor Observatory. Aerosol Air Qual. Res. 20 (4), 663–678.

Lei, X., Bian, J., Xiu, G., Hu, X., Gu, X., Bian, Q., 2017. The mobile monitoring of black carbon and its association with roadside data in the Chinese megacity of Shanghai. Environ. Sci. Pollut. Res. 24, 7482–7489.

Li, B., Lei, X., Xiu, G., Gao, C., Gao, S., Qian, N., 2015. Personal exposure to black carbon during commuting in peak and off-peak hours in Shanghai. Sci. Total Environ. 525, 237–245.

Liu, C., Chung, C.E., Yin, Y., Schnaiter, M., 2018a. The Absorption Ångström Exponent of black carbon: from numerical aspects. Atmos. Chem. Phys. 18 (9), 6259–6273.

Liu, B., Minle, M., Wu, C., Li, J., Li, Y., Ting, N., Zhen, J., Lau, A.K.H., Fung, J.C.H., In, K., Meng, K., Chan, C.K., Jie, Y., 2019a. Potential exposure to fine particulate matter ($PM_{2.5}$) and black carbon on jogging trails in Macau. Atmos. Environ. 198, 23–33.

Liu, M., Peng, X., Meng, Z., Zhou, T., Long, L., She, Q., 2019b. Spatial characteristics and determinants of in-traffic black carbon in Shanghai, China : combination of mobile monitoring and land use regression model. Sci. Total Environ. 658, 51–61.

Liu, Y., Yan, C., Zheng, M., 2018b. Source apportionment of black carbon during winter in Beijing. Sci. Total Environ. 618, 531–541.

Madueño, L., Kecorius, S., Löndahl, J., Müller, T., Pfeifer, S., Haudek, A., Mardoñez, V., Wiedensohler, A., 2019. A new method to measure real-world respiratory tract deposition of inhaled ambient black carbon. Environ. Pollut. 248, 295–303.

Madureira, J., Slezakova, K., Silva, A.I., Lage, B., Mendes, A., Aguiar, L., Pereira, M.C., Teixeira, J.P., Costa, C., 2020. Assessment of indoor air exposure at residential homes: inhalation dose and lung deposition of PM_{10}, $PM_{2.5}$ and ultrafine particles among newborn children and their mothers. Sci. Total Environ. 717, 137293.

Martinello, K., Oliveira, M.L.S., Molossi, F.A., Ramos, C.G., Teixeira, E.C., Kautzmann, R.M., Silva, L.F.O., 2014. Direct identification of hazardous elements in ultra-fine and nanominerals from coal fly ash produced during diesel co-firing. Sci. Total Environ. 470–471.

Martins, J.V., Artaxo, P., Liousse, C., Reid, J.S., Hobbs, P.V., Kaufman, Y.J., 1998. Effects of black carbon content, particle size, and mixing on light absorption by aerosols from biomass burning in Brazil. J. Geophys. Res. Atmos. 103, 32041–32050.

Martinsson, J., Azeem, H.A., Sporre, M.K., Bergström, R., Ahlberg, E., Öström, E., 2017. Carbonaceous aerosol source apportionment using the Aethalometer model – evaluation by radiocarbon and levoglucosan analysis at a rural background site in southern Sweden. Atmos. Chem. Phys. 17, 4265–4281.

Martinsson, J., Eriksson, A.C., Nielsen, I.E., Malmborg, V.B., Ahlberg, E., Andersen, C., Lindgren, R., Nyström, R., Nordin, E.Z., Brune, W.H., Svenningsson, L., Swietlicki, E., Boman, C., Pagels, J.H., 2015. Impacts of combustion conditions and photochemical processing on the light absorption of biomass bombustion aerosol. Environ. Sci. Technol. 49 (24), 14663–14671.

Massabò, D., Caponi, L., Bernardoni, V., Bove, M.C., Brotto, P., Calzolai, G., Cassola, F., Chiari, M., Fedi, M.E., Fermo, P., Giannoni, M., Lucarelli, F., Nava, S., Piazzalunga, A., Valli, G., Vecchi, R., Prati, P., 2015. Multi-wavelength optical determination of black and brown carbon in atmospheric aerosols. Atmos. Environ. 108, 1–12.

Merritt, A.-S., Georgellis, A., Andersson, N., Bedada, G.B., Bellander, T., Johansson, C., 2019. Personal exposure to black carbon in Stockholm, using different intra- urban transport modes. Sci. Total Environ. 674, 279–287.

Morales Betancourt, R., Galvis, B., Balachandran, S., Ramos-Bonilla, J.P., Sarmiento, O.L., Gallo-Murcia, S.M., Contreras, Y., 2017. Exposure to fine particulate, black carbon, and particle number concentration in transportation microenvironments. Atmos. Environ. 157, 135–145.

Mousavi, A., Sowlat, M.H., Lovett, C., Rauber, M., Szidat, S., Boffi, R., Borgini, A., De Marco, C., Ruprecht, A.A., Sioutas, C., 2019. Source apportionment of black carbon (BC) from fossil fuel and biomass burning in metropolitan Milan, Italy. Atmos. Environ. 203, 252–261.

Okokon, E.O., Yli-Tuomi, T., Turunen, A.W., Taimisto, P., Pennanen, A., Vouitsis, I., Samaras, Z., Voogt, M., Keuken, M., Lanki, T., 2017. Particulates and noise exposure during bicycle, bus and car commuting: a study in three European cities. Environ. Res. 154, 181–189.

de Oliveira Alves, N., Brito, J., Caumo, S., Arana, A., de Souza Hacon, S., Artaxo, P., Hillamo, R., Teinilä, K., Batistuzzo de Medeiros, S.R., de Castro Vasconcellos, P., 2015. Biomass burning in the Amazon region: aerosol source apportionment and associated health risk assessment. Atmos. Environ. 120, 277–285.

de Oliveira Alves, N., Matos Loureiro, A.L., dos Santos, F.C., Nascimento, K.H., Dallacort, R., de Castro Vasconcellos, P., de Souza Hacon, S., Artaxo, P., de Medeiros, S.R.B., 2011. Genotoxicity and composition of particulate matter from biomass burning in the eastern Brazilian Amazon region. Ecotoxicol. Environ. Saf. 74 (5), 1427–1433.

de Oliveira Alves, N., Vessoni, A.T., Quinet, A., Fortunato, R.S., Kajitani, G.S., Peixoto, M.S., de Souza Hacon, S., Artaxo, P., Saldiva, P., Menck, C.F.M., Batistuzzo de Medeiros, S.R., 2017. Biomass burning in the Amazon region causes DNA damage and cell death in human lung cells. Sci. Rep. 7, 10937.

de Oliveira Alves, N., Ignotti, E., Artaxo, P., Saldiva, P.H.N., Junger, W.L., Hacon, S., 2012. Risk assessment of $PM_{2.5}$ to child residents in Brazilian Amazon region with biofuel production. Environ. Health 11, 64.

Oliveira, M.L.S., Ward, C.R., French, D., Hower, J.C., Querol, X., Silva, L.F.O., 2012. Mineralogy and leaching characteristics of beneficiated coal products from Santa Catarina, Brazil. Int. J. Coal Geol. 94, 314–325.

Oliveira, M.L.S., Marostega, F., Taffarel, S.R., Saikia, B.K., Waanders, F.B., DaBoit, K., Baruah, B.P., Silva, L.F.O., 2014. Nano-mineralogical investigation of coal and fly ashes from coal-based captive power plant (India): an introduction of occupational health hazards. Sci. Total Environ. 468–469, 1128–1137.

Oliveira, M.L.S., Navarro, O.G., Crissien, T.J., Tutikian, B.F., da Boit, K., Teixeira, E.C., Cabello, J.J., Agudelo-Castañeda, D.M., Silva, L.F.O., 2017. Coal emissions adverse human health effects associated with ultrafine/nano-particles role and resultant engineering controls. Environ. Res. 158, 450–455.

Ozdemir, H., Pozzoli, L., Kindap, T., Demir, G., Mertoglu, B., Mihalopoulos, N., Theodosi, C., Kanakidou, M., Im, U., Unal, A., 2014. Spatial and temporal analysis of black carbon aerosols in Istanbul megacity. Sci. Total Environ. 473–474, 451–458.

Petzold, A., Schloesser, H., Sheridan, P.J., Arnott, W.P., Ogren, J.A., Virkkula, A., 2005. Evaluation of multiangle absorption photometry for measuring aerosol light absorption. Aerosol Sci. Technol. 39 (1), 40–51.

Qiu, Y., Wu, X., Zhang, Y., Xu, L., Hong, Y., Chen, J., Chen, X., Deng, J., 2019. Aerosol light absorption in a coastal city in Southeast China: temporal variations and implications for brown carbon. J. Environ. Sci. 80, 257–266.

Quispe, D., Pérez-López, R., Silva, L.F.O., Nieto, J.M., 2012. Changes in mobility of hazardous elements during coal combustion in Santa Catarina power plant (Brazil). Fuel 94, 495–503.

Rajeevan, K., Sumesh, R.K., Resmi, E.A., Unnikrishnan, C.K., 2019. An observational study on the variation of black carbon aerosol and source identi fi cation over a tropical station in South India. Atmos. Pollut. Res. 10 (1), 30–44.

Ramírez, O., Sánchez de la Campa, A.M., Amato, F., Moreno, T., Silva, L.F., de la Rosa, J.D., 2019. Physicochemical characterization and sources of the thoracic fraction of road dust in a Latin American megacity. Sci. Total Environ. 652, 434–446.

Reddington, C.L., Butt, E.W., Ridley, D.A., Artaxo, P., Morgan, W.T., Coe, H., Spracklen, D.V., 2015. Air quality and human health improvements from reductions in deforestation-related fire in Brazil. Nat. Geosci. 8 (10), 768–771.

Ribeiro, J., Flores, D., Ward, C.R., Silva, L.F.O., 2010. Identification of nanominerals and nanoparticles in burning coal waste piles from Portugal. Sci. Total Environ. 408 (23), 6032–6041.

Ribeiro, J., DaBoit, K., Flores, D., Kronbauer, M.A., Silva, L.F.O., 2013. Extensive FE-SEM/EDS, HR-TEM/EDS and ToF-SIMS studies of micron- to nano-particles in anthracite fly ash. Sci. Total Environ. 452–453, 98–107.

Rojas, J.C., Sánchez, N.E., Schneider, I., Oliveira, M.L.S., Teixeira, E.C., Silva, L.F.O., 2019. Exposure to nanometric pollutants in primary schools: environmental implications. Urban Clim. 27, 412–419.

Saikia, B.K., Ward, C.R., Oliveira, M.L.S., Hower, J.C., Baruah, B.P., Braga, M., Silva, L.F., 2014. Geochemistry and nano-mineralogy of two medium-sulfur northeast Indian coals. Int. J. Coal Geol. 121, 26–34.

Saikia, Binoy K., Saikia, J., Rabha, S., Silva, L.F.O., Finkelman, R., 2018. Ambient nanoparticles/nanominerals and hazardous elements from coal combustion activity: Implications on energy challenges and health hazards. Geosci. Front. 9 (3), 863–875.

Saleh, R., Hennigan, C.J., McMeeking, G.R., Chuang, W.K., Robinson, E.S., Coe, H., Donahue, N.M., Robinson, A.L., 2013. Absorptivity of brown carbon in fresh and photochemically aged biomass-burning emissions. Atmos. Chem. Phys. 13 (15), 7683–7693.

Sandradewi, J., Prévôt, A.S.H., Szidat, S., Perron, N., Alfarra, M.R., Lanz, V.A., Weingartner, E., Baltensperger, U., 2008. Using aerosol light absorption measurements for the quantitative determination of wood burning and traffic emission contributions to particulate matter. Environ. Sci. Technol. 42 (9), 3316–3323.

Saturno, J., Pöhlker, C., Massabò, D., Brito, J., Carbone, S., Cheng, Y., Chi, X., Ditas, F., de Angelis, I.H., Morán-Zuloaga, D., Pöhlker, M.L., Rizzo, L.V., Walter, D., Wang, Q., Artaxo, P., Prati, P., Andreae, M.O., 2017. Comparison of different Aethalometer correction schemes and a reference multi-wavelength absorption technique for ambient aerosol data. Atmos. Meas. Tech. 10 (8), 2837–2850.

Saturno, J., Holanda, B.A., Pöhlker, C., Ditas, F., Wang, Q., Moran-Zuloaga, D., Brito, J., Carbone, S., Cheng, Y., Chi, X., Ditas, J., Hoffmann, T., de Angelis, I.H., Könemann, T., Lavrič, J.V., Ma, N., Ming, J., Paulsen, H., Pöhlker, M.L., Rizzo, L.V., Schlag, P., Su, H., Walter, D., Wolff, S., Zhang, Y., Artaxo, P., Pöschl, U., Andreae, M.O., 2018. Black and brown carbon over Central Amazonia: long-term aerosol measurements at the ATTO site. Atmos. Chem. Phys. 18 (17), 12817–12843.

Schneider, I.L., Teixeira, E.C., Silva Oliveira, L.F., Wiegand, F., 2015. Atmospheric particle number concentration and size distribution in a traffic–impacted area. Atmos. Pollut. Res. 6 (5), 877–885.

Scott, C.E., Monks, S.A., Spracklen, D.V., Arnold, S.R., Forster, P.M., Rap, A., Äijälä, M., Artaxo, P., Carslaw, K.S., Chipperfield, M.P., Ehn, M., Gilardoni, S., Heikkinen, L., Kulmala, M., Petäjä, T., Reddington, C.L.S., Rizzo, L.V., Swietlicki, E., Vignati, E., Wilson, C., 2018. Impact on short-lived climate forcers increases projected warming due to deforestation. Nat. Commun. 9, 157.

Sehn, J.L., de Leão, F.B., da Boit, K., Oliveira, M.L.S., Hidalgo, G.E., Sampaio, C.H., Silva, L.F.O., 2016. Nanomineralogy in the real world: a perspective on nanoparticles in the environmental impacts of coal fire. Chemosphere 147, 439–443.

Shirmohammadi, F., Sowlat, M.H., Hasheminassab, S., Saffari, A., Ban-Weiss, G., Sioutas, C., 2017. Emission rates of particle number, mass and black carbon by the Los Angeles International Airport (LAX) and its impact on air quality in Los Angeles. Atmos. Environ. 151, 82–93.

Silva, L.F.O., Oliveira, M.L.S., Gonçalves, J.O., Dotto, G.L., 2020a. Identification of mercury and nanoparticles in roots with different oxidation states of an abandoned coal mine. Environ. Sci. Pollut. Res. 27 (19), 24380–24386.

Silva, Luis F.O., Crissien, T.J., Schneider, I.L., Blanco, É.P., Sampaio, C.H., 2020b. Nanometric particles of high economic value in coal fire region: opportunities for social improvement. J. Clean. Prod. 256.

Silva, Luis F.O., Milanes, C., Pinto, D., Ramirez, O., Lima, B.D., 2020c. Multiple hazardous elements in nanoparticulate matter from a Caribbean industrialized atmosphere. Chemosphere 239, 124776.

Silva, Luis F.O., Pinto, D., Lima, B.D., 2020d. Implications of iron nanoparticles in spontaneous coal combustion and the effects on climatic variables. Chemosphere 254, 126814.

Singh, V., Ravindra, K., Sahu, L., Sokhi, R., 2018. Trends of atmospheric black carbon concentration over the United Kingdom. Atmos. Environ. 178, 148–157.

Slowik, J.G., Cross, E.S., Han, J.-H., Davidovits, P., Onasch, T.B., Jayne, J.T., Williams, L.R., Canagaratna, M.R., Worsnop, D.R., Chakrabarty, R.K., Moosmüller, H., Arnott, W.P., Schwarz, J.P., Gao, R.-S., Fahey, D.W., Kok, G.L., Petzold, A., 2007. An intercomparison of instruments measuring black carbon content of soot particles. Aerosol Sci. Tech. 41 (3), 295–314.

Stampfer, O., Austin, E., Ganuelas, T., Fiander, T., Seto, E., Karr, C.J., 2020. Use of low-cost PM monitors and a multi-wavelength aethalometer to characterize $PM_{2.5}$ in the Yakama Nation reservation. Atmos. Environ. 224, 117292.

Taheri, A., Aliasghari, P., Hosseini, V., 2019. Black carbon and $PM_{2.5}$ monitoring campaign on the roadside and residential. Atmos. Environ. 116928.

Targino, A.C., Gibson, M.D., Krecl, P., Rodrigues, M.V.C., dos Santos, M.M., de Paula Corrêa, M., 2016. Hotspots of black carbon and $PM_{2.5}$ in an urban area and relationships to traffic characteristics. Environ. Pollut. 218, 1–12.

Targino, A.C., Krecl, P., Danziger Filho, J.E., Segura, J.F., Gibson, M.D., 2018. Spatial variability of on-bicycle black carbon concentrations in the megacity of São Paulo: a pilot study. Environ. Pollut. 242 (A), 539–543.

Titos, G., del Águila, A., Cazorla, A., Lyamani, H., Casquero-Vera, J.A., Colombi, C., Cuccia, E., Gianelle, V., Močnik, G., Alastuey, A., Olmo, F.J., Alados-Arboledas, L., 2017. Spatial and temporal variability of carbonaceous aerosols: assessing the impact of biomass burning in the urban environment. Sci. Total Environ. 578, 613–625.

Van Poppel, M., Peters, J., Bleux, N., 2013. Methodology for setup and data processing of mobile air quality measurements to assess the spatial variability of concentrations in urban environments. Environ. Pollut. 183, 224–233.

Wang, Q., Saturno, J., Chi, X., Walter, D., Lavric, J.V., Moran-Zuloaga, D., Ditas, F., Pöhlker, C., Brito, J., Carbone, S., Artaxo, P., Andreae, M.O., 2016. Modeling investigation of light-absorbing aerosols in the Amazon Basin during the wet season. Atmos. Chem. Phys. 16 (22), 14775–14794.

Wang, Q., Wang, L., Li, X., Xin, J., Liu, Z., Sun, Y., Liu, J., Zhang, J., Du, W., Jin, X., Zhang, T., Liu, S., Liu, Q., Chen, J., Cheng, M., Wang, Y., 2020. Emission characteristics of size distribution, chemical composition and light absorption of particles from field-scale crop residue burning in Northeast China. Sci. Total Environ. 710, 136304.

Weingartner, E., Saathoff, H., Schnaiter, M., Streit, N., Bitnar, B., Baltensperger, U., 2003. Absorption of light by soot particles: determination of the absorption coefficient by means of aethalometers. J. Aerosol Sci. 34 (10), 1445–1463.

Williams, R.D., Knibbs, L.D., 2016. Daily personal exposure to black carbon: a pilot study. Atmos. Environ. 132, 296–299.

Xiao, S., Yu, X., Zhu, B., Kumar, K.R., Li, M., Li, L., 2020. Characterization and source apportionment of black carbon aerosol in the Nanjing Jiangbei New Area based on two years of measurements from Aethalometer. J. Aerosol Sci. 139, 105461.

Zhu, C.S., Cao, J.J., Hu, T.F., Shen, Z.X., Tie, X.X., Huang, H., Wang, Q.Y., Huang, R.J., Zhao, Z.Z., Močnik, G., Hansen, A.D.A., 2017. Spectral dependence of aerosol light absorption at an urban and a remote site over the Tibetan Plateau. Sci. Total Environ. 590–591, 14–21.

Zotter, P., Herich, H., Gysel, M., El-Haddad, I., Zhang, Y., Močnik, G., Hüglin, C., Baltensperger, U., Szidat, S., Prévôt, A.S.H., 2017. Evaluation of the absorption Ångström exponents for traffic and wood burning in the Aethalometer-based source apportionment using radiocarbon measurements of ambient aerosol. Atmos. Chem. Phys. 17 (6), 4229–4249.